HHS Public Access

Author manuscript

Sci Transl Med. Author manuscript; available in PMC 2019 October 03.

Published in final edited form as:

Sci Transl Med. 2018 October 03; 10(461): . doi:10.1126/scitranslmed.aat1445.

p95HER2–T cell bispecific antibody for breast cancer treatment

Irene Rius Ruiz[1,2,*], **Rocio Vicario**[1,*], **Beatriz Morancho**[1,2], **Cristina Bernadó Morales**[1,2], **Enrique J. Arenas**[1], **Sylvia Herter**[3], **Anne Freimoser-Grundschober**[3], **Jitka Somandin**[3], **Johannes Sam**[3], **Oliver Ast**[3], **Águeda Martinez Barriocanal**[1], **Antonio Luque**[1], **Marta Escorihuela**[1], **Ismael Varela**[1], **Isabel Cuartas**[4], **Paolo Nuciforo**[5], **Roberta Fasani**[5], **Vicente Peg**[2,6], **Isabel Rubio**[6], **Javier Cortés**[5], **Violeta Serra**[1,2], **Santiago Escriva-de-Romani**[5,6], **Jeff Sperinde**[7], **Ahmed Chenna**[7], **Weidong Huang**[7], **John Winslow**[7], **Joan Albanell**[2,8,9,10], **Joan Seoane**[2,4,11,12], **Maurizio Scaltriti**[13], **Jose Baselga**[14], **Josep Tabernero**[2,5,6], **Pablo Umana**[3], **Marina Bacac**[3], **Cristina Saura**[5,6,†], **Christian Klein**[3,†], and **Joaquín Arribas**[1,2,11,12,†,‡]

[1]Preclinical Research Program, Vall d'Hebron Institute of Oncology (VHIO), 08035 Barcelona, Spain. [2]Centro de Investigación Biomédica en Red de Cáncer (CIBERONC), 08035 Barcelona, Spain. [3]Roche Innovation Center Zurich, Roche Pharmaceutical Research and Early Development, Wagistrasse 18, 8952 Schlieren, Switzerland. [4]Translational Research Program, VHIO, 08035 Barcelona, Spain. [5]Clinical Research Program, VHIO, 08035 Barcelona, Spain. [6]Vall

[‡]Corresponding author. jarribas@vhio.net.
[*]These authors contributed equally to this work.
[†]These authors jointly supervised this work.

Author contributions: I.R.R. and R.V. designed and performed most experiments, interpreted the data, and revised the manuscript. B.M., E.J.A., and C.B.M. designed, conducted, and interpreted some experiments and revised the manuscript. A.F.-G., J. Sam, J. Somandin, S.H., and O.A. designed and produced p95HER2-TCB. A.M.B., A.L., M.E., and I.V. performed IHC and performed some in vivo experiments. J. Seoane and I.C. performed intracranial injection into humanized mice. P.N. and R.F. evaluated immunohistochemical analyses. V.P., I.R., J.C., V.S., S.E.-d.-R., J.S., A.C., W.H., and J.W. analyzed the expression of p95HER2 in FFPE sections. J. Albanell, M.S., J.B., J.T., P.U., M.B., C.S., and C K. provided critical support and corrected the manuscript. J. Arribas designed the study, interpreted the data, and wrote the manuscript.

Competing interests: A.F.-G., J. Somandin, J. Sam, S.H., O.A., P.U., M.B., and C.K. declare employment with Roche. P.U., M.B., and C.K. declare ownership of Roche stock. V.P. has received consultation fees from Sysmex Spain. I.R. has received honoraria from Roche. J.C. has received honoraria from Roche, Novartis, Eisai, Celgene, and Pfizer and consulting/advisor fees from Roche, Celgene, AstraZeneca, Cellestia Biotech, Biothera, Merus, and Seattle Genetics. V.S. maintains noncommercial research agreements with AstraZeneca, Novartis, Genentech, and Tesaro. S.E.-d.-R. has received honoraria from Roche, Pierre Fabre, Kyowa-Kirin, and Eisai and travel expesenses from Roche and Daiichi Sankyo. J. Sperinde, A.C., W.H., and J.W. are LabCorp employees and owners of LabCorp stock. J. Albanell participates in advisory board meetings for Roche, Pfizer, Amgem, Merck, Sharp & Dohme (MSD) and has received speaking fees from Roche, Pfizer, and Amgen. J. Seoane receives research grants from Roche Glycart, Mosaic Biomedicals, and Ridgeline Therapeutic; is a consultant/advisory board member of Northern Biologicals; and has ownership interest in Mosaic Biomedicals and Northern Biologicals. M.S. received research funds from Puma Biotechnoloy, Daiichi-Sankio, and Menarini Ricerche and is a cofounder of Medendi Medical Travel. J.B. is on the Board of Directors for Varian Medical Systems, Bristol-Myers Squibb, and Foghorn and is a past board member of Grail, Aura Biosciences, and Infinity Pharmaceuticals. He has performed consulting and/or advisory work for Grail, PMV Pharma, ApoGen, Juno, Roche, Lilly, Novartis, and Northern Biologics. He has stock or other ownership interests in PMV Pharma, Grail, Varian, Foghorn, Aura, Infinity, ApoGen, Tango, and Venthera, for which he is a cofounder. He has previously received honoraria or travel expenses from Roche, Novartis, and Lilly. J.T. reports scientific consultancy role for Bayer, Boehringer Ingelheim, Chugai, Genentech Inc., Ipsen, Lilly, MSD, Merck Serono, Merrimack, Merus, Novartis, Peptomyc, Pfizer, Rafael Pharmaceuticals, F. Hoffmann–La Roche Ltd., Sanofi, Symphogen, and Taiho. C.S. has received honoraria for consultancy from Roche/Genentech, AstraZeneca, Puma Biotechnology, Eisai, Pfizer, Novartis, Synthon, Celgene, Daiichi, and Pierre Fabre Iberica and research grants from Roche, AstraZeneca, Puma Biotechnology, and Eisai. J. Arribas has received research funds from Roche, Synthon, Menarini, and Molecular Partners and consultancy honoraria from Menarini. C.K., M.B., A.F.-G., S.H., J. Arribas, and R.V. are inventors on patent application EP16191933.7 held/submitted by Hoffmann–La Roche Inc. that covers p95HER2-TCBs, novel bispecific antigen binding molecules for T cell activation and redirection to specific target cells. All other authors declare that they have no competing interests.

Data and materials availability: All data associated with this study are present in the paper or supplementary materials. All materials will be made available for the scientific community.

d'Hebron University Hospital, 08035 Barcelona, Spain. [7]Monogram Biosciences, Laboratory Corporation of America Holdings, South San Francisco, CA 94080, USA. [8]Cancer Research Program, IMIM (Hospital del Mar Medical Research Institute), 08003 Barcelona, Spain. [9]Medical Oncology Service, Hospital delMar, 08003 Barcelona, Spain. [10]Universitat Pompeu Fabra, 08003 Barcelona, Spain. [11]Department of Biochemistry and Molecular Biology, Universitat Autónoma de Barcelona, Campus de la UAB, 08193 Bellaterra, Spain. [12]Institució Catalana de Recerca i Estudis Avançats, 08010 Barcelona, Spain. [13]Department of Pathology, Human Oncology and Pathogenesis Program, Memorial Sloan Kettering Cancer Center, New York, NY 10065, USA. [14]Department of Medicine, Human Oncology and Pathogenesis Program, Memorial Sloan Kettering Cancer Center, New York, NY 10065, USA.

Abstract

T cell bispecific antibodies (TCBs) are engineered molecules that include, within a single entity, binding sites to the T cell receptor and to tumor-associated or tumor-specific antigens. The receptor tyrosine kinase HER2 is a tumor-associated antigen in ~25% of breast cancers. TCBs targeting HER2 may result in severe toxicities, likely due to the expression of HER2 in normal epithelia. About 40% of HER2-positive tumors express p95HER2, a carboxyl-terminal fragment of HER2. Using specific antibodies, here, we show that p95HER2 is not expressed in normal tissues. We describe the development of p95HER2-TCB and show that it has a potent antitumor effect on p95HER2-expressing breast primary cancers and brain lesions. In contrast with a TCB targeting HER2, p95HER2-TCB has no effect on nontransformed cells that do not overexpress HER2. These data pave the way for the safe treatment of a subgroup of HER2-positive tumors by targeting a tumor-specific antigen.

INTRODUCTION

Strategies to boost the immune response against tumors include two broad categories. One comprises approaches that take advantage of an already existing immune reaction against tumor-specific or tumor-associated antigens. The other is aimed to direct cytotoxic T lymphocytes against tumor cells, independently of the specificity of T cell receptors (TCRs). This can be achieved by generating contacts between cancer cells and cytotoxic T cells through chimeric antigen receptors (CARs) or T cell bispecific antibodies (TCBs), also known as T cell engagers.

CARs consist of the antigen-binding domain of an antibody fused to intracellular signaling motifs that activate T cells (1–3). TCBs are engineered molecules that include, within a single entity, binding sites to the invariant CD3ε chain of the TCR and to a tumor-associated or a tumor-specific antigen. Binding to the tumor antigen results in cross-linking of the TCR and subsequent lymphocyte activation and tumor cell killing (4–6).

One of the main hurdles in the development of CARs or TCBs is the scarcity of extracellularly exposed antigens genuinely specific for tumors, that is, completely absent in nontransformed tissues. Because of this lack of bona fide tumor-specific antigens, the vast majority of CARs or TCBs are directed against tumor-associated antigens. As a result, major

side effects due to redirection of T cells against normal tissues expressing these antigens have been observed (2, 3, 5, 7–9).

To overcome this difficulty, two strategies are conceivable. One consists of adjusting dosages of CARs or TCBs that avoid damaging normal tissues but preserve antitumor activity. The second is to continue the search for tumor antigens not present in normal tissues.

HER2 is a receptor tyrosine kinase overexpressed in different tumors, including ~25% of breast and gastric cancers (10). Both CARs (11, 12) and TCBs (13–15) targeting HER2 have been developed. HER2-CARs not only are effective against HER2-overexpressing cells but also target normal cells expressing HER2 (16). This “on-target off-tumor” effect likely explains fatal adverse effects described in a patient treated with a HER2-CAR. In this patient, T cell activation in the lung, resulting in cardiopulmonary failure, was observed (7). Subsequently, these side effects have been avoided by lowering the doses of newly designed CAR T cells targeting HER2, and clinical trials in which no evident toxicities were observed are currently ongoing (12,17). As an alternative, we looked for a tumor-specific antigen to exclusively target HER2-expressing tumors (“on-target on-tumor” effect) while sparing normal tissues.

About 40% of HER2-positive tumors express p95HER2, a constitutively active C-terminal fragment of HER2. p95HER2 is synthesized by alternative initiation of translation of the transcript encoding the full-length receptor (18). We previously developed different antibodies that recognize p95HER2 but not full-length HER2, likely because they were directed against epitopes exposed in the fragment but not accessible in the native full-length molecule (19, 20). We hypothesized that p95HER2 would be expressed only by cancer cells and, thus, that a TCB antibody recognizing p95HER2 would have anti-tumor effect but would be devoid of the side effects of TCBs recognizing HER2.

RESULTS

Expression of p95HER2 in normal tissues

p95HER2 is expressed in a subset of HER2-positive tumors (18); however, its expression in normal tissues has not been previously analyzed. Using anti-p95HER2–specific antibodies (Fig. 1A), which were previously generated and characterized (*19, 20*), p95HER2 could not be detected in tissue microarrays containing samples from 36 normal adult human tissues. In contrast, and as previously reported (21), full-length HER2 could be readily detected in the epithelia of skin, gastrointestinal, respiratory, reproductive, and urinary tracts (Fig. 1B and fig. S1). Western blot analysis confirmed these results, and whereas HER2 was detected in samples from different tissues, p95HER2 was undetectable (Fig. 1C). We concluded that p95HER2 is a bona fide tumor-specific antigen toward which T cells could be safely redirected.

Generation and characterization of a bispecific antibody against p95HER2 and CD3

We constructed a TCB against p95HER2 (p95HER2-TCB) using an anti-p95HER2 antibody (19). The epitope recognized by the anti-p95HER2 antibody, PIWKFPD, is located 34 amino acids from the plasma membrane (fig. S2A). The corresponding mouse sequence

(PIWKYPD, fig. S2B) was recognized by the anti-p95HER2 with very low affinity (fig. S2, C and D), despite the minimal difference from the human sequence (F to Y amino acid change).

p95HER2-TCB consists of an asymmetric two-armed immunoglobulin G1 (IgG1) that binds monovalently to CD3e and bivalently to p95HER2 (Fig. 2A). The advantage of this design is, on one hand, the monovalent low affinity of the free bispecific antibody for CD3ε (ca. 70 to 100 nM) (22), which disfavors T cell binding and activation in the absence of binding to p95HER2. On the other hand, this bi-specific antibody binds bivalently to the tumor antigen, making use of avidity. A direct comparison of this 2:1 TCB design with different 1:1 designs has shown the superiority of the former (22). In addition, the Fc of p95HER2-TCB was engineered by introducing P329G LALA mutations to avoid binding to the Fcγ receptor (23).

The binding affinity of p95HER2-TCB for p95HER2 is ca. 9 nM, very similar to that of the original anti-p95HER2 antibody (fig. S3). To further characterize p95HER2-TCB, we analyzed its binding to the Jurkat human T lymphocyte cell line, to human peripheral blood mononuclear cells (PBMCs), and to MCF10A cells (which are derived from normal human breast epithelium) transfected with constructs expressing HER2 and/or p95HER2. The results confirmed the specificity of p95HER2-TCB and the relatively low and high affinities for CD3 and p95HER2, respectively (Fig. 2B). Note that p95HER2 migrates as a slow–migrating, fully glycosylated form and an immature form (Fig. 2C) (24).

Despite the clear preference for binding to cells expressing p95HER2 (Fig. 2B, right), p95HER2-TCB also bound to HER2-overexpressing MCF10A cells (Fig. 2D). This residual binding could be due to interaction with the full-length receptor or, alternatively, to low expression of p95HER2 in cells overexpressing HER2. Because p95HER2 is synthesized from the mRNA encoding HER2 through alternative initiation of translation from the AUG codon encoding methionine-611 (24), we analyzed the binding of p95HER2-TCB to cells expressing a complementary DNA construct with a methionine-to-alanine mutation in position 611. The results showed that the binding of p95HER2-TCB to cells overexpressing HER2 is largely due to the generation of p95HER2 synthesized by alternative initiation of translation from methionine-611 (Fig. 2, E and F). These data highlight the specificity of p95HER2-TCB.

For functional analyses, we co-incubated MCF10A cells expressing HER2 and/or p95HER2 with PBMCs and different concentrations of p95HER2-TCB (Fig. 2G). The original anti-p95HER2 antibody or p95HER2-TCB had no effect on MCF10A/ p95HER2 cells in the absence of PBMCs (fig. S4A), indicating that attenuation of p95HER2 signaling did not contribute to the effect of the TCB. At low concentrations (≤10 nM) of p95HER2-TCB, lymphocytes displayed markers of activation only in the presence of cells expressing p95HER2 (Fig. 2H and figs. S4B and S5). Accordingly, lymphocytes killed only cells expressing p95HER2 (Fig. 2I). The analysis of effector molecules such as interleukin-2 (IL-2), granzyme B, and interferon-γ (IFN-γ), produced by activated lymphocytes, confirmed the ability of p95HER2-TCB to induce the cytotoxic killing of cells expressing p95HER2 (Fig. 2J).

Effect of p95HER2-TCB in vivo

MCF10A cells do not grow as xenografts in mice. Thus, to assess the efficacy of p95HER2-TCB in vivo, we generated MCF7 cells expressing p95HER2. Because p95HER2 expression induces senescence in these cells through the up-regulation of the cyclin-dependent kinase inhibitor p21 (25), we knocked down this factor to obtain proliferating MCF7 cells expressing p95HER2 (fig. S6A). Coculture experiments with these cells, PBMCs, and p95HER2-TCB confirmed the efficacy of p95HER2- TCB in vitro (fig. S6, B to D).

A common methodology to assay immune therapies in vivo involves the transplantation of PBMCs into immunocompromised mice carryingxenografted tumor cells (Fig.3A) (26). However, components of the class I histocompatibility complex can be strong alloantigens and be recognized as distinct targets by T cells. Thus, the degree of histocompatibility may determine the degree of tumor rejection in this experimental system. In agreement with this fact, PBMCs from different donors had different effects on the growth of MCF7 p95HER2 cells as xenografts (fig. S7A). Despite these differences, compared with a nontargeting control TCB, p95HER2-TCB had a potent antitumor effect, independently of the source of PBMCs (Fig.3, B and C, and fig. S7B). Supporting the efficacy and specificity of p95HER2-TCB, we did not detect human lymphocyte engraftment, defined as circulating cells positive for human CD45, in the outlier mouse bearing a tumor that showed a growth rate similar to those of mice treated with vehicle or nontargeting TCB (fig. S7C). The percentage of tumor cells, measured by positivity against an anti-cytokeratin antibody (Fig.3D), was significantly lower ($P < 0.001$) after treatment with p95HER2-TCB, showing that volume likely overestimates tumor burden in p95HER2-TCB–treated mice.

At the end of the experiment, the percentages of circulating human $CD8^+$ cells were similar in the three groups of mice (Fig. 3E, blood). In contrast, tumors in mice treated with p95HER2-TCB contained a higher percentage of $CD8^+$ lymphocytes (Fig.3E,tumor).

Current therapies targeting HER2, such as trastuzumab, are effective against extracranial HER2-positive tumors, but their efficacy against brain metastases remains limited (27, 28). Therefore, there is a need to develop drugs for patients with HER2-positive brain lesions. To test the efficacy of p95HER2-TCB on these lesions, we used immunodeficient mice humanized with hematopoietic stem cells (Fig 3F). To generate this model, $CD34^+$ cells obtained from human cord blood were injected into 5-week-old immunodeficient mice (29). After 4 to 5 months, >30% of cells in peripheral blood from these mice were positive for human CD45, which means that they were of human origin (Fig.3G). Next, MCF7 p95HER2 cells expressing luciferase were inoculated into the brains of these mice. Bioluminescence monitoring showed the efficacy of p95HER2-TCB against the intracranial tumors (Fig.3, G to I).

The lack of efficacy of trastuzumab on brain lesions is attributed to poor transport through the blood-brain barrier (BBB) (28). To test the ability of p95HER2-TCB to cross the BBB, we used an in vitro model (fig. S8A). As expected, in this model, trastuzumab poorly crossed a barrier composed of BBB components and had a limited effect on target cells, even in the presence of PBMCs (fig. S8B). In contrast, in the presence of PBMCs, p95HER2-

TCB effectively reached target cells (fig. S8, C and D), probably because lymphocytes with bound p95HER2-TCB crossed this BBB in vitro model.

Effect of HER2-TCB and p95HER2-TCB on nontransformed cells expressing HER2

To directly compare the redirection of T cells via p95HER2 and HER2, we used a trastuzumab-based HER2-TCB with a 2:1 structure identical to that of p95HER2-TCB. In line with the expression data shown in Fig. 1, HER2-TCB, but not p95HER2-TCB, bound to the surface of nontransformed MCF10A cells or to normal epithelial cells (NECs) obtained from reduction mammoplasties (Fig. 4A, left). Accordingly, coculture experiments showed that HER2-TCB, but not p95HER2-TCB, induced the activation ofcytotoxic lymphocytes and target cell killing (Fig. 4A, middle and right).

Therapies directed against HER2 may contribute to cardiac toxicity [(30) and references therein]. Coculture experiments showed that human cardiomyocytes were effectively killed by HER2-TCB, whereas p95HER2-TCB did not have an effect on these cells (Fig. 4B). Thus, p95HER2-TCB does not affect nontransformed cells, whereas HER2-TCB induces the cytotoxic destruction of the same cells.

In line with this conclusion, HER2-TCB, but not p95HER2-TCB, induced regression of tumors generated by parental MCF7 cells, which do not overexpress HER2 (fig. S9A). Of note, the efficacy of HER2-TCB on parental MCF7 cells and on the same cells overexpressing HER2 was similar. Thus, low expression of HER2 already triggered effective target cell killing, and this effect was not increased by higher HER2 expression (fig. S9).

Defining a threshold of effectivity

A quantitative IHC-based assay (20) showed that the amounts of p95HER2 in breast tumors vary by more than two orders of magnitude (31, 32). To find the concentration of p95HER2 necessary to trigger the activation of lymphocytes mediated by p95HER2-TCB, we used a panel of HER2-positive patient-derived xenografts (PDXs).

Expression of p95HER2 in samples from original tumors and the corresponding PDXs was similar. In p95HER2-positive tumors (H score ≥ 145), >80% of the cells were positive for p95HER2 both in the original tumor and in the corresponding PDX (Fig. 5A and fig. S10). Thus, during expansion in immunodeficient mice, expression of p95HER2 by tumor cells remained largely invariable.

To quantify the activation of T cells induced by p95HER2-TCB in the presence of cells from different PDXs, we used Jurkat cells expressing an NFAT (nuclear factor of activated T cells)–driven reporter of TCR activation coupled to luciferase (Fig. 5B). Using two PDXs previously characterized as high (PDX67) and low (PDX118) expressers of p95HER2 (33), we showed that increasing concentrations of p95HER2-TCB resulted in TCR activation in co-cultures with cells from the high-expresser p95HER2 PDX (Fig. 5C). A similar analysis was performed on eight additional HER2-positive PDXs and, as controls, on two PDXs established from triple-negative breast cancers (PDX284 and PDX347) (Fig. 5D).

As expected, there was a positive correlation between the activation of the TCR induced by p95HER2-TCB and the amount of p95HER2 determined by the quantitative IHC-based assay (20) (Fig. 5E), IHC, and Western blot (fig. S10). These results allowed us to establish a threshold of p95HER2 expression above which p95HER2-TCB induces activation of the TCR: ~24 relative fluorescence (RF)/mm^2, as judged by the VeraTag assay, and H score ~145, as judged by IHC (Fig. 5E and fig S10C).

Effect of p95HER2-TCB on PDXs

To confirm the results obtained with the Jurkat cells expressing the reporter of TCR activation, we used an in vivo approach. Using PBMCs from the same patient who donated the tumor to establish PDX173, we observed a clear anti-tumor effect of p95HER2-TCB, in vitro and in vivo (Fig. 6A, matched). Using PBMCs from an unrelated healthy donor, p95HER2-TCB also had a clear antitumor effect (Fig. 6A, nonmatched), despite the fact that these allogeneic PBMCs had some cytotoxic effect on PDX173, both in vitro and in vivo (Fig. 6A, compare matched and nonmatched PBMCs in assays with vehicle).

Positivity to anti-cytokeratin confirmed that most of the remaining tumors in p95HER2-TCB–treated mice contained few tumor cells. Analysis of $CD8^+$ lymphocytes confirmed the ability of p95HER2-TCB to increase infiltration of T cells into tumors (fig. S11).

To confirm these results, we also used mice humanized with $CD34^+$ cells (Fig. 6, B and C). In this model, treatment with p95HER2-TCB also impaired tumor growth (Fig. 6D) and promoted the infiltration by $CD8^+$ lymphocytes and their activation (Fig. 6E).

Finally, we analyzed the effect of p95HER2-TCB in two additional $HER2^+$ PDXs, PDX251G and PDX445, which expressed p95HER2 above and below the threshold necessary for the activation of the TCR mediated by p95HER2-TCB, respectively (Fig. 5D). The results confirmed that the quantitative analysis of p95HER2 expression is useful to predict the antitumor activity of p95HER2-TCB, because treatment was only effective in the PDX with p95HER2 expression above the defined threshold (Fig. 7).

DISCUSSION

One major drawback of redirecting T lymphocytes against tumor cells via tumor-associated antigens is the undesired effect on healthy tissues. Because tumor-associated antigens recognized by engineered molecules (CARs or TCBs) are frequently also expressed in normal tissues, on-target off-tumor effects caused by redirected lymphocytes can be severe or even fatal.

The expression of HER2 is readily detectable in normal epithelial tissues (21). In fact, current drugs targeting HER2, such as the monoclonal antibody trastuzumab or the tyrosine kinase inhibitor lapatinib, induce cardiotoxicity in patients, particularly in combination with chemotherapy. This effect is likely due to the expression of HER2 in cardiomyocytes (30). The expression in normal tissues is also the likely reason for the side effects observed with CARs and TCBs targeting HER2 (7, 16). To avoid these undesired effects, doses of CAR T cells against HER2 have been lowered, from 10^{10} cells (7) to 10^8 cells (12). Although these

doses are safe (12, *15, 34*), they may compromise the antitumor effect of the treatment. We have followed an alternative approach by developing a TCB against p95HER2, a truncated form of HER2 that is undetectable in NECs.

An additional advantage of p95HER2 as a target for TCBs stems from its short extracellular domain. The proximity of the plasma membrane to the epitope recognized in tumor cells by TCBs facilitates T cell synapse formation and, thus, tumor cell lysis (35). The peptide recognized by p95HER2-TCB is located only 34 amino acids from the plasma membrane, and this proximity likely contributes to its efficacy.

Thus, p95HER2 is expected to be a safe target for the redirection of T cells against tumor cells and the efficient lysis of the latter. Our results fully support these expectations. Although p95HER2-TCB had a potent effect on tumors expressing p95HER2, we did not detect any effect on cells with low HER2 expression or even on HER2- amplified, p95HER2-negative tumors.

Arguably, side effects due to on-target off-tumor redirection of T lymphocytes via tumor-associated antigens can be more efficiently controlled with TCBs than with CAR T cells. The administration of TCBs can be stopped at will, should side effects become intolerable. In addition, the dose of TCB can be easily gauged to find a safe therapeutic window. However, such a window may represent a compromise that sacrifices maximal antitumor effect to preserve the integrity of normal tissues. The use of truly tumor-specific antigens, such as p95HER2, to redirect lymphocytes will help to increase the dose of TCB to achieve maximal antitumor effect without side effects.

One serious limitation of current anti-HER2 drugs is their lack of efficacy against brain metastases. In the case of trastuzumab, this inefficacy is attributed to its inefficient penetration through the BBB (28). In our experimental setting, p95HER2-TCB effectively impaired the growth of intracranially implanted cells, indicating that cytotoxic lymphocytes can be redirected against brain metastases. In vitro analyses indicated that although p95HER2-TCB itself does not efficiently cross the BBB, $CD3^+$ lymphocytes can transport p95HER2-TCB to reach intracranial tumors. Given the limitations of in vitro BBB models, this hypothesis should be tested in the future in vivo, using immune-competent models.

As an aside, it is currently unclear how allogeneic reactions affect experimental models aimed to reconstitute the interplay between tumor and immune cells. In our analyses, we included human leukocyte antigen (HLA)–matched and nonmatched lymphocytes and confirmed that allogeneic PBMCs may reject tumors and thus using these cells can complicate the interpretation of some experiments. Despite this complication in all experiments performed, p95HER2-TCB had a clear effect on p95HER2-positive cells, irrespective of the source of PBMCs.

In summary, p95HER2 is a bona fide tumor-specific antigen expressed by a subset of HER2-positive breast cancers and, thus, redirecting T cells toward p95HER2 is likely a safe and effective antitumor immune therapy.

MATERIALS AND METHODS

Study design

This study was designed to validate p95HER2 as a safe target toward which T cells can be effectively redirected using a bispecific antibody, p95HER2-TCB. We assessed p95HER2-TCB effectiveness using in vitro and in vivo assays combining human cell lines or patient-derived models with human lymphocytes. For in vitro studies, a minimum of two biological replicates were performed. For in vivo models, we used two sources of immune cells: (i) PBMCs, either patient-matched or nonmatched, and (ii) $CD34^+$ hematopoietic stem cells. All human samples were obtained following institutional guidelines under protocols approved by the institutional review boards (IRBs) at Vall d'Hebron Hospital. Animal work was performed according to protocols approved by the Ethical Committee for the Use of Experimental Animals at the Vall d'Hebron Institute of Oncology. For in vivo experiments, three to seven mice were used per treatment group, and they were randomized by tumor size. Mice that died before the end of the experiment for reasons unrelated to treatment or that did not have detectable percentages of human immune cells were excluded. Because of ethical reasons, we ended experiments before the full development of graft-versus-host disease or when tumor volume surpassed 1000 mm^3. Experiments were not performed in a blinded fashion.

Cell lines and primary cultures

MCF7 (#HTB-22), MCF10A (#CRL-10317), and Jurkat cells (#TIB-152) were from the American Type Culture Collection. MCF7 Tet On cell line was generated by lentiviral transduction of pTRIPZ-p95HER2 vector, generated by a modification of the pTRIPZ vector (Open Biosystems, Thermo Fisher Scientific) to allow p95HER2 overexpression, and pTRIPZ-shp21. pTRIPZ-shp21 was generated by cloning shp21 sequence from pGIPZ CDKN1A short hairpin RNA from Open Biosystems–Thermo Fisher Scientific (RHS4430–200281172 clone V3LHS-322234) into pTRIPZ vector. MCF7-HER2 stably overexpressing cells were generated with retroviral pBabe-hygro vector. MCF10A cells stably expressing vector, p95HER2, HER2, or the combination were generated by retroviral (pQCXIH or pQCXIH-HER2) and lentiviral (pLEX or pLEX-p95HER2) infection. Jurkat-Lucia NFAT cells (#SL0032) were from Signosis.

Cell cultures derived from PDXs were maintained in Dulbecco's modified Eagle's medium/F12 supplemented with 1% L-glutamine, 1% penicillin/streptomycin, and 1% insulin-transferrin-selenium-ethanolamine (#51500056, Life Technologies).

Tumor samples

Human breast tumors used in this study were from biopsies or surgical resections at Vall d'Hebron University Hospital, Barcelona, and were obtained following institutional guidelines. The IRBs at Vall d'Hebron Hospital provided approval for this study in accordance with the Declaration of Helsinki. Written informed consent was obtained from all patients who provided tissue and/or blood.

Patient-derived xenografts

Fragments of patient samples were implanted into the fat pad of NOD. CB17-Prkdcscid [nonobese diabetic (NOD)/severe combined immuno-deficient (SCID)] (#SM-NOD-5S-F, Janvier) or NOD.Cg-PrkdcscidIl2rgtm1WjI/SzJ NOD scid gamma (NSG) (#005557, Charles River Laboratories) mice, and 17β-estradiol (1 μM) (#E8875–1G, Sigma-Aldrich) was added to drinking water. Tumor xenografts were measured with calipers three times per week, and tumor volume was determined using the following formula: (length x width^2) x (π/6).

Proliferation assay

Cells (1×10^5 per well) were seeded in 96-well plates. At the indicated times, cells were detached with trypsin-EDTA, and viable cells were determined by trypan blue dye exclusion and counted on a Neubauer chamber.

Western blot

Primary antibodies recognizing HER2 (c-ERBB-2) (CB11, #MU134-UCE, BioGenex), human glyceraldehyde-3-phosphate dehydrogenase (GAPDH) (#Ab128915, Abcam), and p21 (#Ab11CP74, NeoMarkers) were used. As secondary antibodies, we used enhanced chemilumi-nescence (ECL) rabbit IgG, horseradish peroxidase (HRP)–linked whole antibody (from donkey, #NA934–1ML, Amersham GE Healthcare) and ECL mouse IgG, HRP-linked whole antibody (from sheep, #NA931, Amersham GE Healthcare).

PBMC isolation

PBMCs were isolated from pre-analyzed buffy coats obtained from healthy donors through the Blood and Tissue Bank of Catalonia (Banc de Sang i Teixits) or peripheral blood from patients. Blood was diluted with 1x phosphate-buffered saline (PBS), 2:1, and transferred to 50-ml tubes with Ficoll-Paque PLUS (#70–1440-02, GE Healthcare) at a 4:3 ratio, following the manufacturer's protocol.

Cytotoxicity assays and T cell activation

All target cells were harvested with StemPro Accutase, counted, and seeded in 96-well flat bottom plates. Effector PBMCs were added 24 hours later to each well in a proportion of 10:1 in RPMI1640,2% fetal bovine serum (FBS). Serial dilutions of the indicated antibodies were performed in RPMI 1640, 2% FBS medium and added to the target/effector-containing wells. The plates were incubated for 48 hours, and LDH release was determined with the CytoTox 96 Non-Radioactive Cytotoxicity Assay (#G1780, Promega).

PBMCs from cytotoxicity and cytokine release assays were resuspended in 1x PBS, 2.5 mM EDTA, 1% bovine serum albumin (BSA), and 5% horse serum. Twenty minutes later, samples were centrifuged and cells were incubated for 45 min with the following anti-body mix: hCD8 phycoerythrin (PE)-Cy7 (#344712), hCD4 BV421 (#317434), hCD25 allophycocyanin (APC) (#302610), and hCD69 fluorescein isothiocyanate (FITC) (#310904), all from BioLegend at a 1:300 dilution. After a wash with 1x PBS, samples were acquired on LSR Fortessa (BD Biosciences).

Cytokine analysis

Fifty microliters of supernatant was collected and transferred to a 96-well plate for granzyme B, IFN-γ, and IL-2 detection with the CBA Human Soluble Protein Flex Set (#558264, BD Biosciences) as indicated by the manufacturer.

Analysis of HER2 and p95HER2 expression in tissue microarrays

Tissue microarrays, MNO1021 and ab178227, were purchased from Biomax and Abcam, respectively. MN0102 and ab178227 were probed with the anti-p95HER2 antibody described in (33). All samples were clearly negative. MNO1021 and ab178227 were also probed with anti-HER2 (c-ERBB-2) (CB11, #MU134-UCE, BioGenex).

Cardiomyocyte cytotoxicity assay and T cell activation in vitro

Cardiomyocytes (iCell Cardiomyocytes, Cellular Dynamics #CMC-100–110-00) were cultured according to the supplier's instructions. For the assessment of T cell activation, surface staining for CD8 (APC anti-human CD8, BD #55536), CD4 (FITC anti-human CD4, BioLegend #300506), CD69 (BV421 anti-human CD69, BioLegend #310930), and CD25 (PE-Cy7 anti-human CD25, BioLegend #302612) was performed according to the suppliers' indications. Samples were analyzed using a BD FACSCanto II.

Jurkat-luciferase assay

Tumors derived from PDXs were excised and cut into the smallest pieces possible, incubated for 1 hour with collagenase 1A (200 U/ml; #C9891, Sigma-Aldrich), washed, filtered through 100-μm strainers (#352360, Corning), and counted. Single target cells were cocultured with effector Jurkat-Lucia cells at a 5:1 effector/target (E:T) ratio. Luciferase signal was measured using the Luciferase Assay System (#E1501, Promega) and following the manufacturer's protocol.

Cell survival assay

Tumors derived from PDXs were excised and digested as described above. Cell suspension was plated in 40-μl dots of Matrigel (#354234, Corning) in 48-well flat plates. Once organotypic cell cultures were established, organoids were digested to single cells. Then, cells were labeled with CFSE (#C34554, Invitrogen) according to the manufacturer's protocol. CFSE-labeled cells (derived from PDXs or MCF7-p95HER2) were cocultured with PBMCs from healthy donors or matched patients at an E:T ratio 10:1 in the presence of 50 nM p95HER2-TCB or vehicle in 96-well V-bottom plates. After 72 hours of incubation, the mixture of cells was washed with 1x PBS and resuspended in 1x PBS, 2.5 mM EDTA, 1% BSA, and 5% horse serum for 20 min. Then, cells were stained with hCD8 PE-Cy7, hCD4 BV421, hCD25 APC, and hCD69 APC-Cy7 (#310913, BioLegend), all used at a 1:300 dilution. Zombie Aqua (#423101, BioLegend) was used as a viability marker at a 1:1000 dilution. CFSE-positive cells were counted, and the percentage of corresponding leukocytes was measured on LSR Fortessa and analyzed with FlowJo software.

Humanized xenograft models

NSG mice were injected orthotopically with 3×10^6 MCF7-p95HER2 cells or implanted with approximately 3 × 3 mm tumor fragments. Once tumor volume reached 200 mm^3, animals were intraperitoneally injected with 10^7 PBMCs obtained from healthy donors or matched patients. After 48 hours, animals were treated biweekly with p95HER2-TCB (1 mg/kg), nontargeting TCB, or vehicle intravenously. In the case of MCF7 p95HER2 cells, mice were maintained in the presence of doxycycline (1 g/liter) in the drinking water.

To obtain immunodeficient mice with a reconstituted human immune system, $CD34^+$ cells were purified from human cord blood obtained through the Blood and Tissue Bank of Catalonia. These cells were intravenously injected into 5-week-old NSG mice previously treated intraperitoneally with busulfan (15 mg/kg) to ablate the hematopoietic system of the mouse. After 4 to 5 months, the percentages of circulating human $CD45^+$ cells were determined, and mice containing >30% $hCD45^+$ in peripheral blood were orthotopically implanted with about 3 × 3 mm tumor fragments. Once tumors reached 200 mm^3, animals were randomized and treated biweekly with p95HER2-TCB (1 mg/kg) or vehicle (intravenously).

At the end of the experiment, mouse blood and tumors were analyzed. Tumors were cut into small pieces and digested in collagenase IA (200 U/ml) and deoxyribonuclease I (1 μg/ml) in RPMI medium. After 1 hour of incubation at 37°C with shaking at 80 rpm, the mixture was filtered through 100-μm strainers. Red blood cell lysis was performed in digested tumors and blood samples. After a wash with PBS, the cells from tumor and blood were resuspended in PBS, 2.5 mM EDTA, 1% BSA, and 5% horse serum for 20 min. Then, cells were stained with hCD45 PE (#304008), msCD45 AF488 (#103122), hCD3 peridinin chlorophyll protein (PerCP)-Cy5.5 (#300430), hCD8 PE-Cy7, hCD4 BV421, and hCD25 APC, hCD69 FITC, all used at a 1:300 dilution. Zombie Aqua (#423101, BioLegend) was used as a viability marker at a 1:1000 dilution. Samples were acquired on LSR Fortessa and analyzed with FlowJo software. Box plots show the percentage of the indicated live leukocytes ($CD45^+$ or $CD8^+$). Lower and higher whiskers indicate 10th and 90th percentiles, respectively; lower and higher edges of the box indicate 25 th and 75 th percentiles, respectively; the inner line in the box indicates 50th percentile.

Intracranial tumor assay

MCF7 p95HER2 cells (5×10^5) transduced with the lentiviral vector pLENTI CMV V5-Luc Blast (MCF7 p95HER2/luc cells) were stereotactically inoculated in the brains of NSG mice humanized with $CD34^+$ cells as described above, in the presence of doxycycline (1 g/liter) in the drinking water. The rate of tumor growth was monitored by in vivo bioluminescence imaging with the IVIS-200 Imaging System from Xenogen (PerkinElmer).

Quantitative p95 assay (VeraTag)

p95HER2 was quantified using the VeraTag platform and a monoclonal antibody against p95HER2 that does not recognize full-length HER2, as previously described in (20).

Immunohistochemical analysis

PDXs or human breast cancer sample tissues were fixed in 4% formaldehyde buffered to pH 7 (stabilized with methanol) for 24 hours and were then formalin-fixed and paraffin-embedded (FFPE). Tissue sections of 4 μm thickness were mounted on positively charged glass slides and immunostained with the indicated antibodies. A certified pathologist, R.F., evaluated p95HER2 expression by histoscore (H score) (36),a semiquantitative assessment of intensity of staining (graded as follows: 0, nonstaining; 1, weak; 2, median; or 3, strong, using adjacent normal tissue as reference) and the percentage of positive cells. R.F. also calculated the percentages of cytokeratin- and CD8-positive cells.

Normal tissue lysates

Tissue lysates obtained from normal colon, liver, uterus, heart, breast, and esophagus were purchased from Amsbio.

Transmigration BBB assay

A BBB model was generated using hCMEC/D3 cells, brain micro-vascular endothelial cells that maintain phenotypic features of BBB(37) and have been used to model BBB in vitro [for example, see(38)]. Cells were cultured in precoated collagen I (rat tail, Gibco, A1048301, 150 μg/ml) plates, with EGM2 medium + bulletkit factors (CC-3156 and CC-4176, Lonza), accordingto the manufacturer's instructions. To generate the BBB model, 3-μm transwells (3-mm polyester transwells, Costar #3472) were coated with collagen I (150 μg/ml) for 2 hours and then coated with fibronectin (10 μg/ml; Sigma-Aldrich, FF1141) for 1 hour. After coating, transwells were washed with 1x PBS twice, and 100,000 of hCMEC/D3 cells were seeded on top of the transwells to generate the BBB components. When cells reached confluency (3 to 5 days), they were starved overnight in starving EGM2 medium, and target cells were seeded in the low chamber. For cytotoxic assays, cells were cultured for 72 hours and CFSE counts were analyzed by flow cytometry.

Surface plasmon resonance

Surface plasmon resonance measurements were performed on a Biacore T200 (GE Healthcare). Anti-p95HER2 IgG and TCB were captured on the sensor chip surface by a chemically immobilized anti-human Fc IgG (GE Healthcare, BR-1008–39). The p95Her2 peptide (MPIWKFPDEEGAKKKK, synthesized at Bachem) was used as an analyte (300 to 0.14 nM serial dilution), and the sensor chip surface was regenerated with 3 M $MgCl_2$ between single injections. Kinetic evaluation was performed by global fitting of the data to a 1:1 interaction model.

Statistical analyses

GraphPad Prism 6.0 was used for statistical analyses. For in vitro experiments, comparisons between two groups were made by Student's *t* test. For in vivo experiments, we used two-way ANOVA with subsequent Bonferroni correction. We did not use statistical methods to predetermine sample size in animal studies, but we did make efforts to achieve the scientific goals using the minimum number of animals. A sample size of three to seven mice per group was chosen on the basis of our previous experience. Original data are provided in table S1.

Supplementary Material

Refer to Web version on PubMed Central for supplementary material.

Acknowledgments:

NECs obtained from reduction mammoplasties were provided by L.Tusell (Cell Biology Unit, Department of Cell Biology, Physiology and Immunology, Bioscience School, Universitat Autònoma de Barcelona, Bellaterra, Spain). hCMEC/D3 cells were a gift from A. Rosell 's laboratory (Vall d 'Hebron Institute of Research).

Funding: Supported by grants of the Breast Cancer Research Foundation (BCRF-17–008), Spanish Association Against Cancer, Agéncia de Gestió d 'Ajuts Universitaris i de Recerca (AGAUR) and European Regional Development Fund (2016 PROD 00108), FERO Foundation and Instituto de Salud Carlos III (PI16/00253 and CB16/12/00449) to J. Arribas. The work of J. Arribas, J.T., J.B., and M.S. was funded by the Comprehensive Program of Cancer Immunotherapy and Immunology (CAIMI) supported by the Banco Bilbao Vizcaya Argentaria Foundation (FBBVA) (grant 89/2017) and NIH grants P30CA008748 and R01CA190642–01 (J.B.) and the Breast Cancer Research Foundation. J. Seoane is supported by Instituto de Salud Carlos III (PI16/01278). I.R.R. is supported by a fellowship from AGAUR-FI-DGR. B.M. is supported by a fellowship from PERIS (Departament de Salut, Generalitat de Catalunya) and the FERO Foundation. J. Seoane, V.S., and J. Arribas are members of EuroPDX.

REFERENCES AND NOTES

1. Gross G, Waks T, Eshhar Z, Expression of immunoglobulin-T-cell receptor chimeric molecules as functional receptors with antibody-type specificity. Proc. Natl. Acad. Sci. U.S.A. 86, 10024–10028 (1989). [PubMed: 2513569]
2. Klebanoff CA, Rosenberg SA, Restifo NP, Prospects for gene-engineered T cell immunotherapy for solid cancers. Nat. Med. 22, 26–36 (2016). [PubMed: 26735408]
3. Lim WA, June CH, The principles of engineering immune cells to treat cancer. Cell 168, 724–740 (2017). [PubMed: 28187291]
4. Staerz UD, Kanagawa O, Bevan MJ, Hybrid antibodies can target sites for attack by T cells. Nature 314, 628–631 (1985). [PubMed: 2859527]
5. Garber K, Bispecific antibodies rise again. Nat. Rev. Drug Discov. 13, 799–801 (2014). [PubMed: 25359367]
6. Del Bano J, Chames P, Baty D, Kerfelec B, Taking up cancer immunotherapy challenges: Bispecific antibodies, the path forward? Antibodies 5, 1–23 (2016).
7. Morgan RA, Yang JC, Kitano M, Dudley ME, Laurencot CM, Rosenberg SA, Case report of a serious adverse event following the administration of T cells transduced with a chimeric antigen receptor recognizing ERBB2. Mol. Ther. 18, 843–851 (2010). [PubMed: 20179677]
8. Abken H, Driving CARs on the highway to solid cancer: Some considerations on the adoptive therapy with CAR T cells. Hum. Gene Ther. 28, 1047–1060 (2017). [PubMed: 28810803]
9. Weiner GJ, Building better monoclonal antibody-based therapeutics. Nat. Rev. Cancer 15, 361–370 (2015). [PubMed: 25998715]
10. Slamon DJ, Clark GM, Wong SG, Levin WJ, Ullrich A, McGuire WL, Human breast cancer: Correlation of relapse and survival with amplification ofthe HER-2/neu oncogene. Science 235, 177–182 (1987). [PubMed: 3798106]
11. Zhao Y, Wang QJ, Yang S, Kochenderfer JN, Zheng Z, Zhong X, Sadelain M, Eshhar Z, Rosenberg SA, Morgan RA, A herceptin-based chimeric antigen receptor with modified signaling domains leads to enhanced survival of transduced T lymphocytes and antitumor activity. J. Immunol. 183, 5563–5574 (2009). [PubMed: 19843940]
12. Ahmed N, Brawley VS, Hegde M, Robertson C, Ghazi A, Gerken C, Liu E, Dakhova O, Ashoori A, Corder A, Gray T, Wu M-F, Liu H, Hicks J, Rainusso N, Dotti G, Mei Z, Grilley B, Gee A, Rooney CM, Brenner MK, Heslop HE, Wels WS, Wang LL, Anderson P, Gottschalk S, Human epidermal growth factor receptor 2 (HER2) -specific chimeric antigen receptor-modified T cells for the immunotherapy of HER2-positive sarcoma. J. Clin. Oncol. 33, 1688–1696 (2015). [PubMed: 25800760]

13. Kiewe P, Hasmüller S, Kahlert S, Heinrigs M, Rack B, Marmé A, Korfel A, Jäger M, Lindhofer H, Sommer H, Thiel E, Untch M, Phase I trial ofthe trifunctional anti-HER2 x anti-CD3 antibody ertumaxomab in metastatic breast cancer. Clin. Cancer Res. 12, 3085–3091 (2006). [PubMed: 16707606]

14. Junttila TT, Li J, Johnston J, Hristopoulos M, Clark R, Ellerman D, Wang B-E, Li Y, Mathieu M, Li G, Young J, Luis E, Lewis Phillips G, Stefanich E, Spiess C, Polson A, Irving B, Scheer JM, Junttila MR, Dennis MS, Kelley R, Totpal K, Ebens A, Antitumor efficacy of a bispecific antibody that targets HER2 and activates T cells. Cancer Res. 74, 5561–5571 (2014). [PubMed: 25228655]

15. Wermke M, Schmidt H, Nolte H, Ochsenreither S, Back J, Salhi Y, Bayever E, A phase I study of the bispecific antibody T-cell engager GBR 1302 in subjects with HER2-positive cancers. J. Clin. Oncol. 35, TPS3091 (2017).

16. van der Stegen SJC, Davies DM, Wilkie S, Foster J, Sosabowski JK, Burnet J, Whilding LM, Petrovic RM, Ghaem-Maghami S, Mather S, Jeannon J-P, Parente-Pereira AC, Maher J, Preclinical in vivo modeling of cytokine release syndrome induced by ErbB-retargeted human T cells: Identifying a window of therapeutic opportunity? J. Immunol. 191, 4589–4598 (2013). [PubMed: 24062490]

17. Liu X, Jiang S, Fang C, Yang S, Olalere D, Pequignot EC, Cogdill AP, Li N, Ramones M, Granda B, Zhou L, Loew A, Young RM, June CH, Zhao Y, Affinity-tuned ErbB2 or EGFR chimeric antigen receptor T cells exhibit an increased therapeutic index against tumors in mice. Cancer Res. 75, 3596–3607 (2015). [PubMed: 26330166]

18. Arribas J, Baselga J, Pedersen K, Parra-Palau JL, p95HER2 and breast cancer. Cancer Res. 71, 1515–1519 (2011). [PubMed: 21343397]

19. Parra-Palau JL, Pedersen K, Peg V, Scaltriti M, Angelini PD, Escorihuela M, Mancilla S, Sánchez Pla A, Ramón y Cajal S, Baselga J, Arribas J, A major role of p95/611-CTF, a carboxy-terminal fragment of HER2, in the down-modulation ofthe estrogen receptor in HER2-positive breast cancers. Cancer Res. 70, 8537–8546 (2010). [PubMed: 20978202]

20. Sperinde J, Jin X, Banerjee J, Penuel E, Saha A, Diedrich G, Huang W, Leitzel K, Weidler J, Ali SM, Fuchs E-M, Singer CF, Köstler WJ, Bates M, Parry G, Winslow J, Lipton A, Quantitation of p95HER2 in paraffin sections by using a p95-specific antibody and correlation with outcome in a cohort of trastuzumab-treated breast cancer patients. Clin. Cancer Res. 16, 4226–4235 (2010). [PubMed: 20664024]

21. Press MF, Cordon-Cardo C, Slamon DJ, Expression of the HER-2/neu proto-oncogene in normal human adult and fetal tissues. Oncogene 5, 953–962 (1990). [PubMed: 1973830]

22. Bacac M, Colombetti S, Herter S, Sam J, Perro M, Chen S, Bianchi R, Richard M, Schoenle A, Nicolini V, Diggelmann S, Limani F, Schlenker R, Hüsser T, Richter W, Bray-French K, Hinton HJ, Giusti AMF, Freimoser-Grundschober A, Lariviére L, Neumann C, Klein C, Umaña P, CD20-TCB with obinutuzumab pretreatment as next generation treatment of hematological malignancies. Clin. Cancer Res. (2018).

23. Schlothauer T, Herter S, Koller CF, Grau-Richards S, Steinhart V, Spick C, Kubbies M, Klein C, Umaña P, Mössner E, Novel human IgG1 and IgG4 Fc-engineered antibodies with completely abolished immune effector functions. Protein Eng. Des. Sel. 29, 457–466 (2016). [PubMed: 27578889]

24. Pedersen K, Angelini P-D, Laos S, Bach-Faig A, Cunningham MP, Ferrer-Ramón C, Luque-García A, García-Castillo J, Parra-Palau JL, Scaltriti M, Ramón y Cajal S, Baselga J, Arribas J, A naturally occurring HER2 carboxy-terminal fragment promotes mammary tumor growth and metastasis. Mol. Cell. Biol. 29, 3319–3331 (2009). [PubMed: 19364815]

25. Angelini PD, Zacarias Fluck MF, Pedersen K, Parra-Palau JL, Guiu M, Bernadó Morales C, Vicario R, Luque-García A, Navalpotro NP, Giralt J, Canals F, Gomis RR, Tabernero J, Baselga J, Villanueva J, Arribas J, Constitutive HER2 signaling promotes breast cancer metastasis through cellular senescence. Cancer Res. 73,450–458 (2013). [PubMed: 23288917]

26. Byrne AT, Alférez DG, Amant F, Annibali D, Arribas J, Biankin AV, Bruna A, Budinská E, Caldas C, Chang DK, Clarke RB, Clevers H, Coukos G, Dangles-Marie V, Eckhardt SG, Gonzalez-Suarez E, Hermans E, Hidalgo M, Jarzabek MA, de Jong S, Jonkers J, Kemper K, Lanfrancone L, Mælandsmo GM, Marangoni E, Marine J-C, Medico E, Norum JH, Palmer HG, Peeper DS, Pelicci PG, Piris-Gimenez A, Roman-Roman S, Rueda OM, Seoane J, Serra V, Soucek L,

Vanhecke D, Villanueva A, Vinolo E, Bertotti A, Trusolino L, Interrogating open issues in cancer precision medicine with patient-derived xenografts. Nat. Rev. Cancer 17, 254–268 (2017). [PubMed: 28104906]

27. Stemmler H-J, Schmitt M, Willems A, Bernhard H, Harbeck N, Heinemann V, Ratio of trastuzumab levels in serum and cerebrospinal fluid is altered in HER2-positive breast cancer patients with brain metastases and impairment of blood-brain barrier. Anticancer Drugs 18, 23–28 (2007). [PubMed: 17159499]
28. Kodack DP, Askoxylakis V, Ferraro GB, Fukumura D, Jain RK, Emerging strategies for treating brain metastases from breast cancer. Cancer Cell 27, 163–175 (2015). [PubMed: 25670078]
29. Rongvaux A, Takizawa H, Strowig T, Willinger T, Eynon EE, Flavell RA, Manz MG, Human hemato-lymphoid system mice: Current use and future potential for medicine. Annu. Rev. Immunol. 31, 635–674 (2013). [PubMed: 23330956]
30. Valachis A, Nearchou A, Polyzos NP, Lind P, Cardiac toxicity in breast cancer patients treated with dual HER2 blockade. Int. J. Cancer 133, 2245–2252 (2013). [PubMed: 23629633]
31. Duchnowska R, Sperinde J, Chenna A, Haddad M, Paquet A, Lie Y, Weidler JM, Huang W, Winslow J, Jankowski T, Czartoryska-Artukowicz B, Wysocki PJ, Foszczyńska-Kłoda M, Radecka B, Litwiniuk MM, Zok J, Wiśniewski M, Zuziak D, Biernat W, Jassem J, Quantitative measurements oftumoral p95HER2 protein expression in metastatic breast cancer patients treated with trastuzumab: Independent validation ofthe p95HER2 clinical cutoff. Clin. Cancer Res. 20, 2805–2813 (2014). [PubMed: 24668646]
32. Scaltriti M, Nuciforo P, Bradbury I, Sperinde J, Agbor-Tarh D, Campbell C, Chenna A, Winslow J, Serra V, Parra JL, Prudkin L, Jimenez J, Aura C, Harbeck N, Pusztai L, Ellis C, Eidtmann H, Arribas J, Cortes J, de Azambuja E, Piccart M, Baselga J, High HER2 expression correlates with response to the combination of lapatinib and trastuzumab. Clin. Cancer Res. 21, 569–576 (2015). [PubMed: 25467182]
33. Parra-Palau JL, Morancho B, Peg V, Escorihuela M, Scaltriti M, Vicario R, Zacarias-Fluck M, Pedersen K, Pandiella A, Nuciforo P, Serra V, Cortés J, Baselga J, Perou CM, Prat A, Rubio IT, Arribas J, Effect of p95HER2/611CTF on the response to trastuzumab and chemotherapy. J. Natl. Cancer Inst. 106, dju291 (2014).
34. Wuellner U, Klupsch K, Buller F, Attinger-Toller I, Santimaria R, Zbinden I, Henne P, Grabulovski D, Bertschinger J, Brack S, Bispecific CD3/HER2 targeting FynomAb induces redirected T cell-mediated cytolysis with high potency and enhanced tumor selectivity. Antibodies 4, 426–440 (2015).
35. Li J, Stagg NJ, Johnston J, Harris MJ, Menzies SA, DiCara D, Clark V, Hristopoulos M, Cook R, Slaga D, Nakamura R, McCarty L, Sukumaran S, Luis E, Ye Z, Wu TD, Sumiyoshi T, Danilenko D, Lee GY, Totpal K, Ellerman D, Hötzel I, James JR, Junttila TT, Membrane-proximal epitope facilitates efficient T cell synapse formation by Anti-FcRH5/CD3 and is a requirement for myeloma cell killing. Cancer Cell 31, 383–395 (2017). [PubMed: 28262555]
36. Hirsch FR, Varella-Garcia M, Bunn PA Jr., Di Maria MV, Veve R, Bremmes RM, Barón AE, Zeng C, Franklin WA, Epidermal growth factor receptor in non-small-cell lung carcinomas: Correlation between gene copy number and protein expression and impact on prognosis. J. Clin. Oncol. 21 , 3798–3807 (2003). [PubMed: 12953099]
37. Poller B, Gutmann H, Krähenbühl S, Weksler B, Romero I, Couraud P-O, Tuffin G, Drewe J, Huwyler J, The human brain endothelial cell line hCMEC/D3 as a human blood-brain barrier model fordrug transport studies. J. Neurochem. 107,1358–1368 (2008). [PubMed: 19013850]
38. Strazza M, Maubert ME, Pirrone V, Wigdahl B, Nonnemacher MR, Co-culture model consisting of human brain microvascular endothelial and peripheral blood mononuclear cells. J. Neurosci. Methods 269, 39–45 (2016). [PubMed: 27216631]

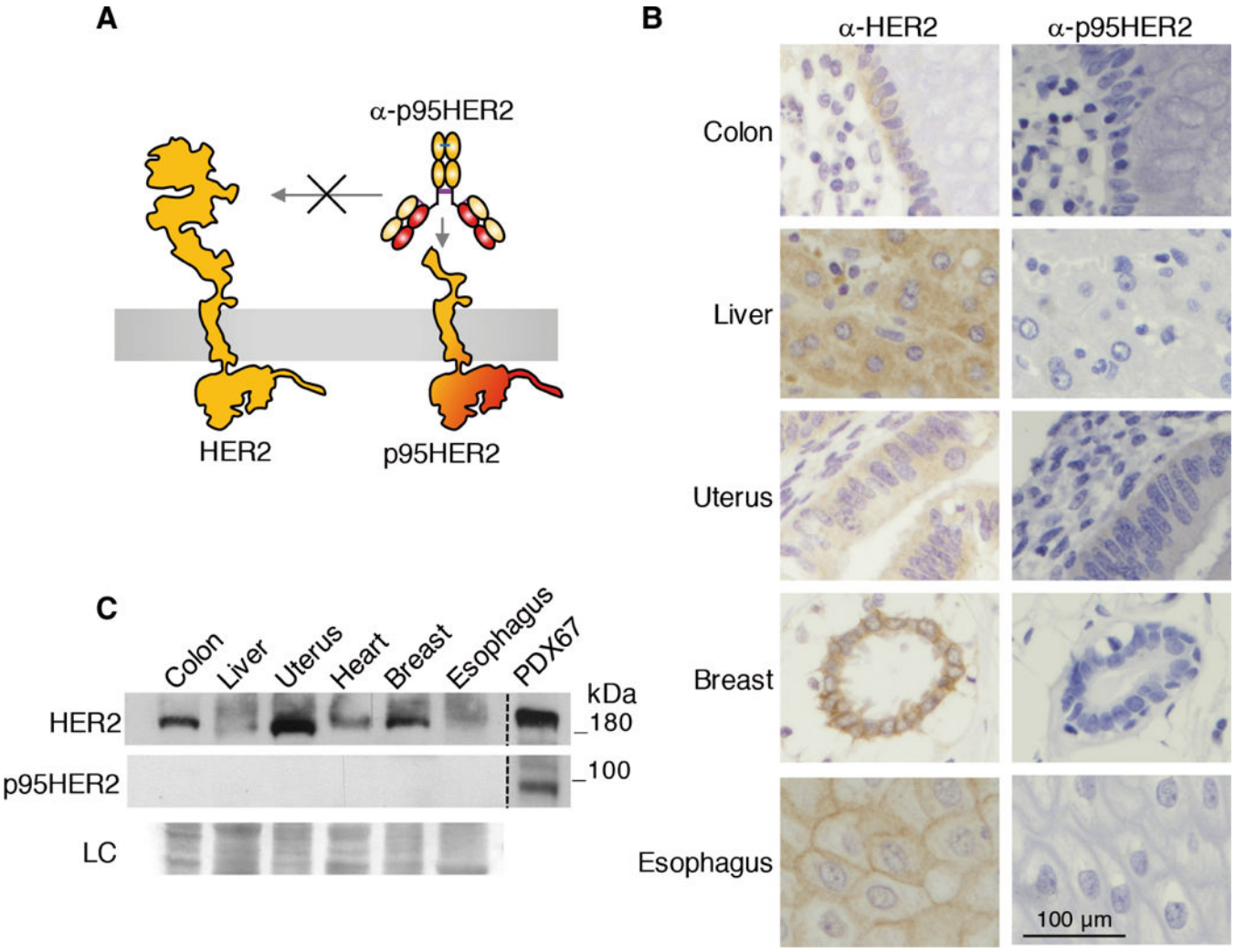

Fig. 1. Expression of p95HER2 in normal tissues.

(**A**) Schematic illustrating the specificity of the anti-p95HER2 antibodies used in this study. (**B**) Immunohistochemical analyses of the expression of HER2 and p95HER2 in the indicated human epithelia. (**C**) Lysates from the indicated normal human tissues were analyzed by Western blot with antibodies against the C terminus of HER2. As a reference for the electrophoretic migration of HER2 and p95HER2, we used lysates from a PDX expressing HER2 and p95HER2 (PDX67). Ponceau staining is shown as loading control (LC).

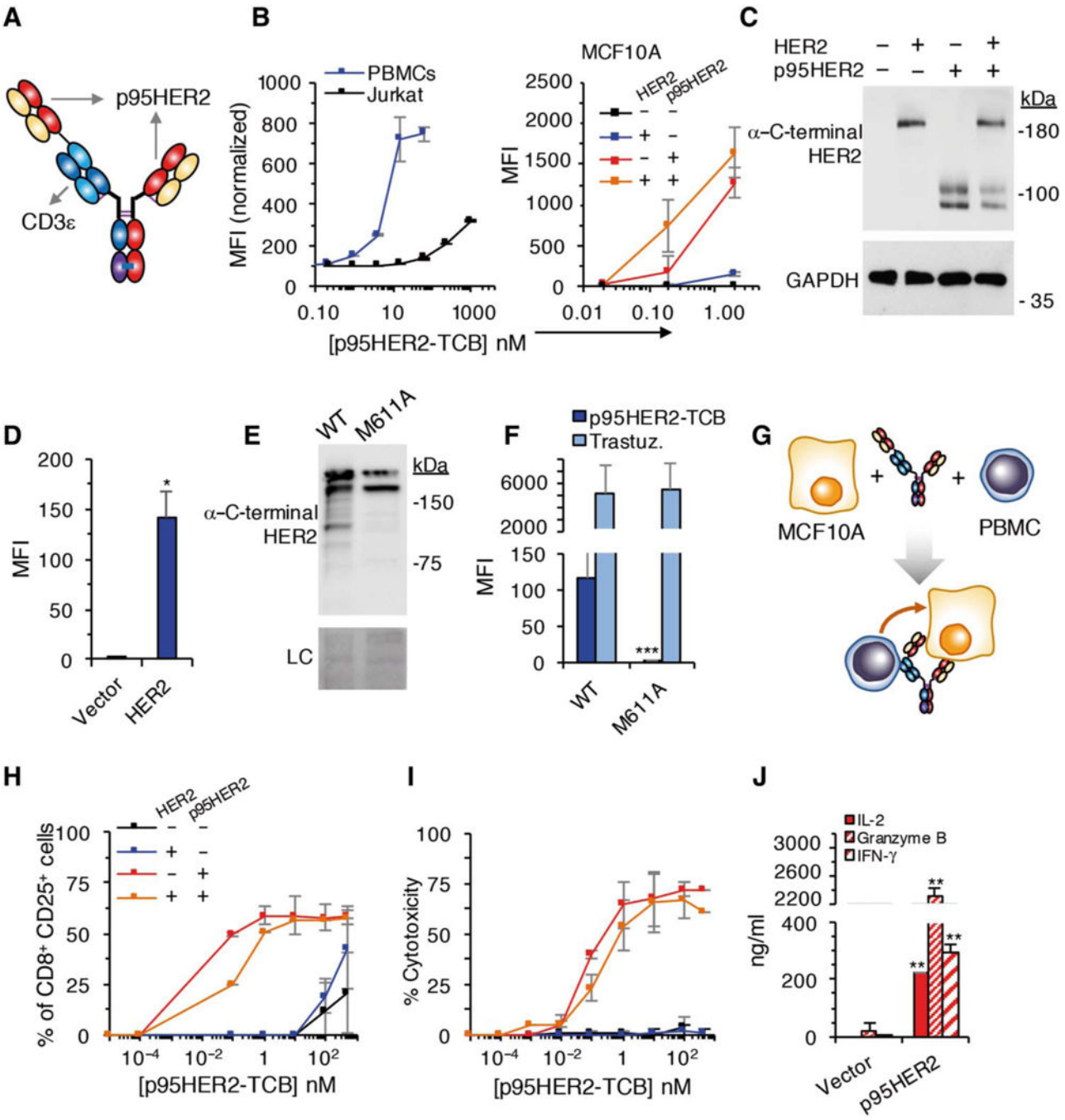

Fig. 2. Characterization of p95HER2-TCB.

(**A**) Schematic showing the structure of p395HER2-TCB. (**B**) Median fluorescence intensity (MFI) of binding of p95HER2-TCB to human Jurkat cells and PBMCs (left) or MCF10A cells expressing empty vector or the same vector encoding HER2 and/or p95HER2 (right) (*n* = 3 expressed as means ± SD, measured by flow cytometry). (**C**) The same MCF10A cells as in (B) (right) expressing the indicated constructs were analyzed by Western blotting with antibodies directed against the C terminus of HER2. (**D**)MFI ofbindingofp95HER2-TCB to control MCF10A cells or the same cells over-expressing full-length HER2 *(n* = 3 expressed

as means ± SD). (**E**) Lysates from MCF10A cells transfected with wild-type (WT) HER2 or HER2 bearing an M611A mutation were analyzed by Western blotting with anti-HER2 antibodies. Ponceau staining is shown as loading control (LC). (**F**) The same cells as in (E) were analyzed by flow cytometry with the indicated antibodies ($n = 3$ expressed as means ± SD). (**G**) Schematic drawing illustrating the coculture experiments to monitor the activity of p95HER2-TCB. (**H** and **I**) MCF10A cells transfected with the indicated vectors were incubated with PBMCs and different concentrations of p95HER2-TCB for 48 hours. Then, the expression of the activation marker CD25 on $CD8^+$ cells was assessed by flow cytometry (H), and cyto-toxicity was determined by measuring lactate dehydrogenase (LDH) release (I) ($n = 3$ expressed as means ± SD). (**J**) MCF10A p95HER2 cells were incubated with PBMCs and 10 nM p95HER2-TCB, and the production of the indicated factors was determined by enzyme-linked immunosorbent assay ($n = 3$ expressed as means ± SD). (D, F, and J) $^*P < 0.05$, $^{**}P < 0.01$, $^{***}P < 0.001$, two-tailed *t* test.

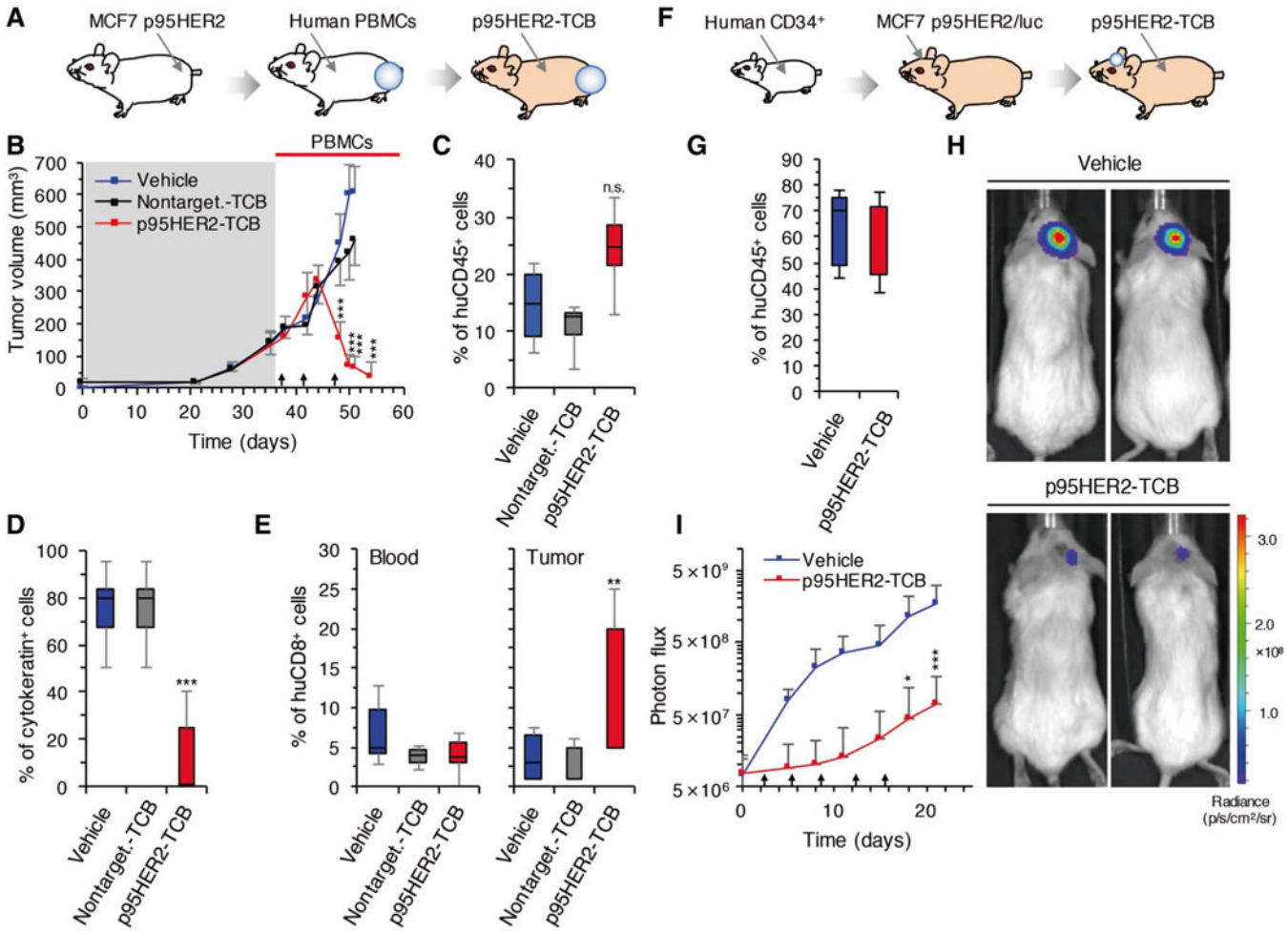

Fig. 3. Effect of p95HER2-TCB on tumor growth in vivo.

(**A**) Schematic drawing illustrating humanization of mice with PBMCs and orthotopic implantation of MCF7 p95HER2 cells. (**B**) Mice were treated with vehicle (control) or nontargeting TCB (1 mg/kg) or p95HER2-TCB (1 mg/kg) (arrows). Tumor volumes, expressed as means ± SD, are shown ($n \geq 7$ per group). (**C**) Percentage of circulating human CD45$^+$, relative to total leukocytes, at the end of the experiment shown in (B). (**D**) Cells positive for cytokeratin were quantified in tumors by immunohistochemistry (IHC). (**E**) Percentages of circulating (blood) and intratumoral (tumor) human CD8$^+$ at the end of the experiment shown in (B). Percentages in blood were calculated by flow cytometry and are relative to total leukocytes. Percentages in tumors were calculated by IHC and are relative to tumor cells. (**F**) Schematic drawing illustrating humanization of mice with CD34$^+$ cells and intracranial injection of MCF7 p95HER2/luciferase cells. (**G**) Percentages of circulating human CD45$^+$ cells, relative to total leukocytes, were determined 5 months after injection of CD34$^+$ cells into NSG mice. (**H** and **I**) Intracranial tumor growth was monitored by assessing bioluminescence (H). Results (I) are expressed as means ± SD ($n \geq 4$ per group). *$P < 0.05$, **$P < 0.01$, ***$P < 0.001$, two-way analysis of variance (ANOVA) and Bonferroni correction (B and I) and two-tailed t test (C to E). In all cases, we compared the group treated with vehicle with the group treated with p95HER2-TCB. n.s., not significant.

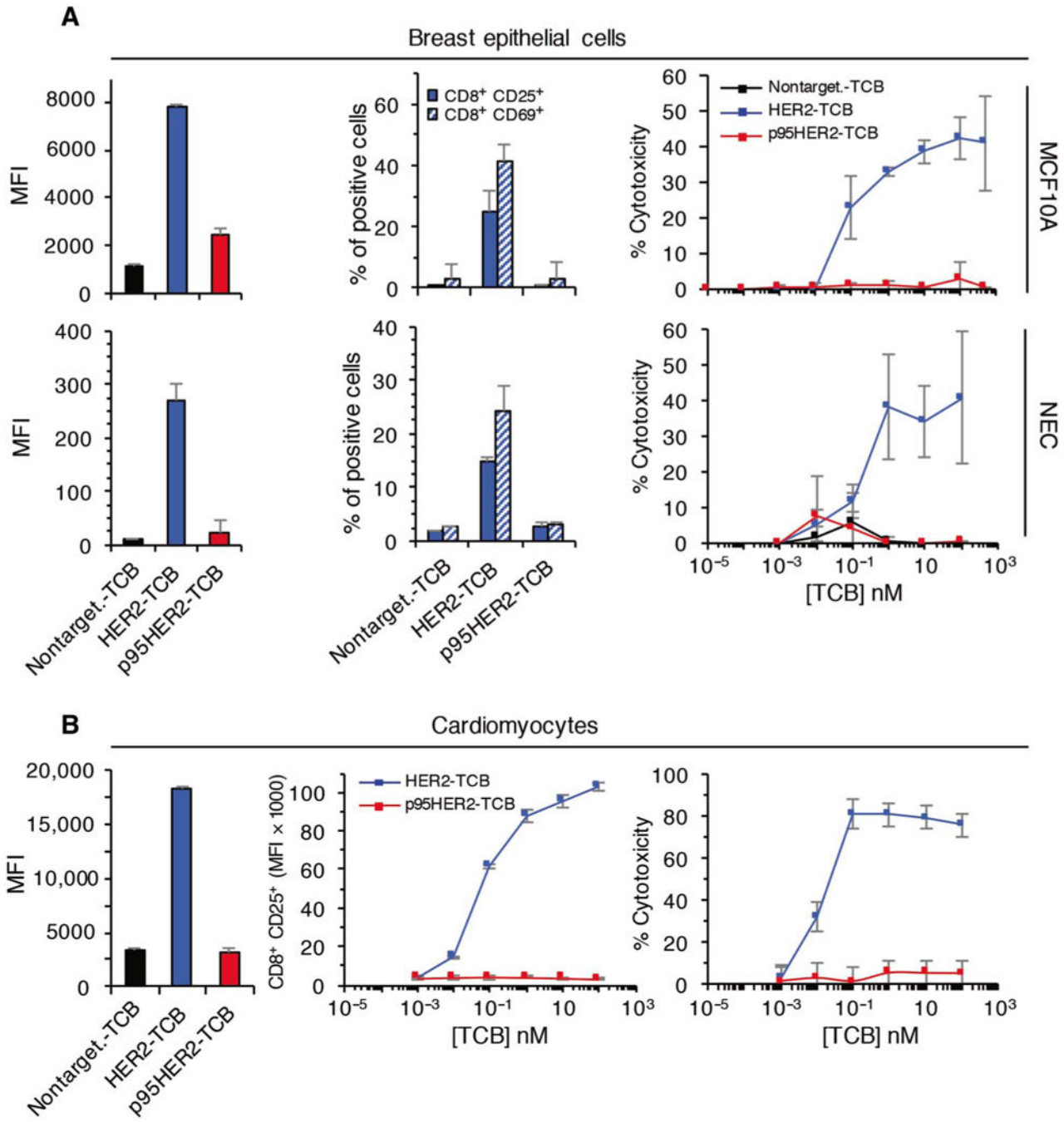

Fig. 4. Effect of HER2-TCB and p95HER2-TCB on nontransformed cells.

MCF10A cells, NECs from reduction mammoplasties (**A**), or human cardiomyocytes (**B**) were cultured with PBMCs from healthy donors for 48 hours, and the effect of p95HER2-TCB was analyzed as in Fig. 2 ($n = 3$ expressed as means ± SD).

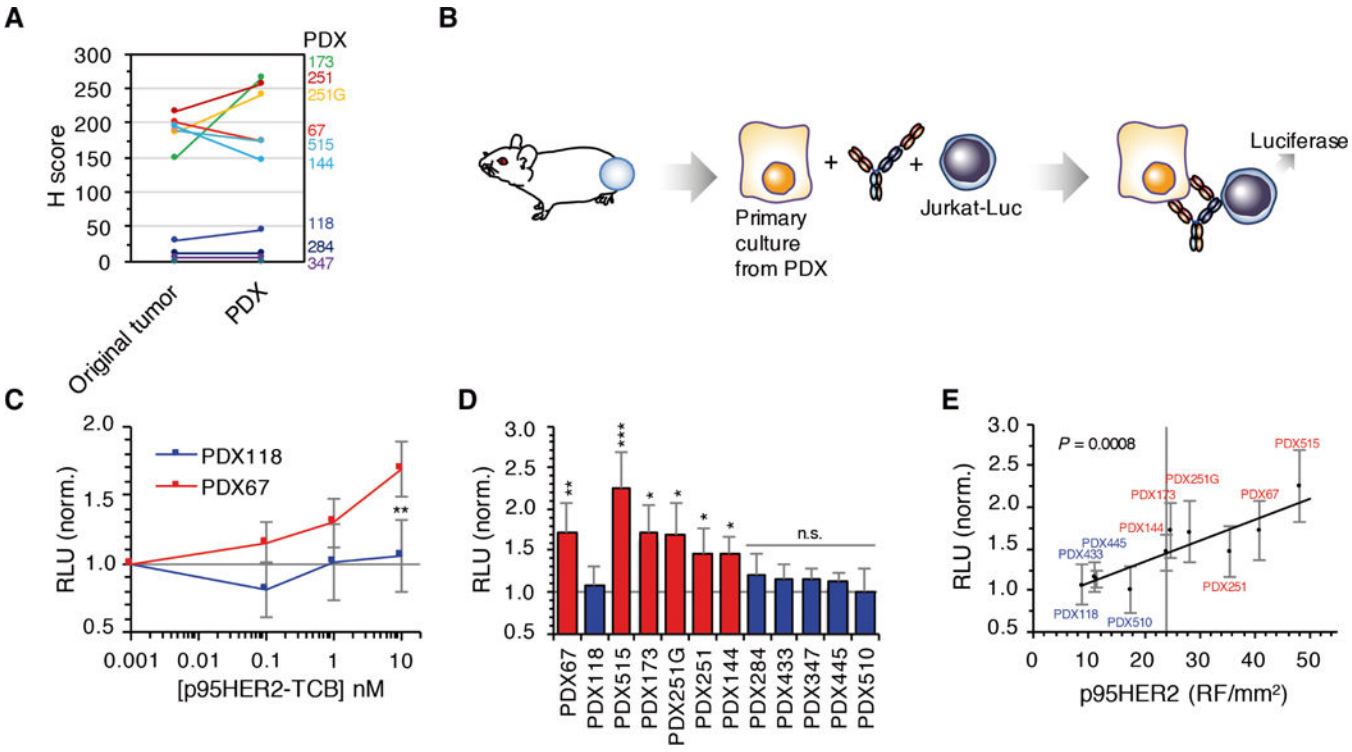

Fig. 5. Effect of p95HER2 expression on the efficacy of p95HER2-TCB.

(**A**) p95HER2 expression in tumor samples and corresponding PDXs was determined by IHC with specific antibodies. (**B**) Schematic drawing illustrating the coculture experiments. (**C**) Cells from PDXs 118 and 67 (negative and positive for p95HER2, respectively) were cocultured in the presence ofthe indicated concentrations of p95HER2-TCB, with Jurkat cells expressing a luciferase-based reporter for the activation of theTCR. Relative luminescence units (RLU) were assessed and normalized to nontargeting TCB ($n = 6$ expressed as means ± SD). (**D**) Cultures from the indicated PDXs were analyzed as in (C) with 10 nM p95HER2-TCB. Statistics compare the results obtained with the different cultures with those obtained with the p95HER2-negative PDX118 ($n \geq 3$ expressed as means ± SD). (**E**) Results obtained in (D) were plotted against the amount of p95HER2 determined using a quantitative IHC-based assay (20). (C and D) $^{*}P < 0.05$, $^{**}P < 0.01$, $^{***}P < 0.001$, two-tailed *t* test.

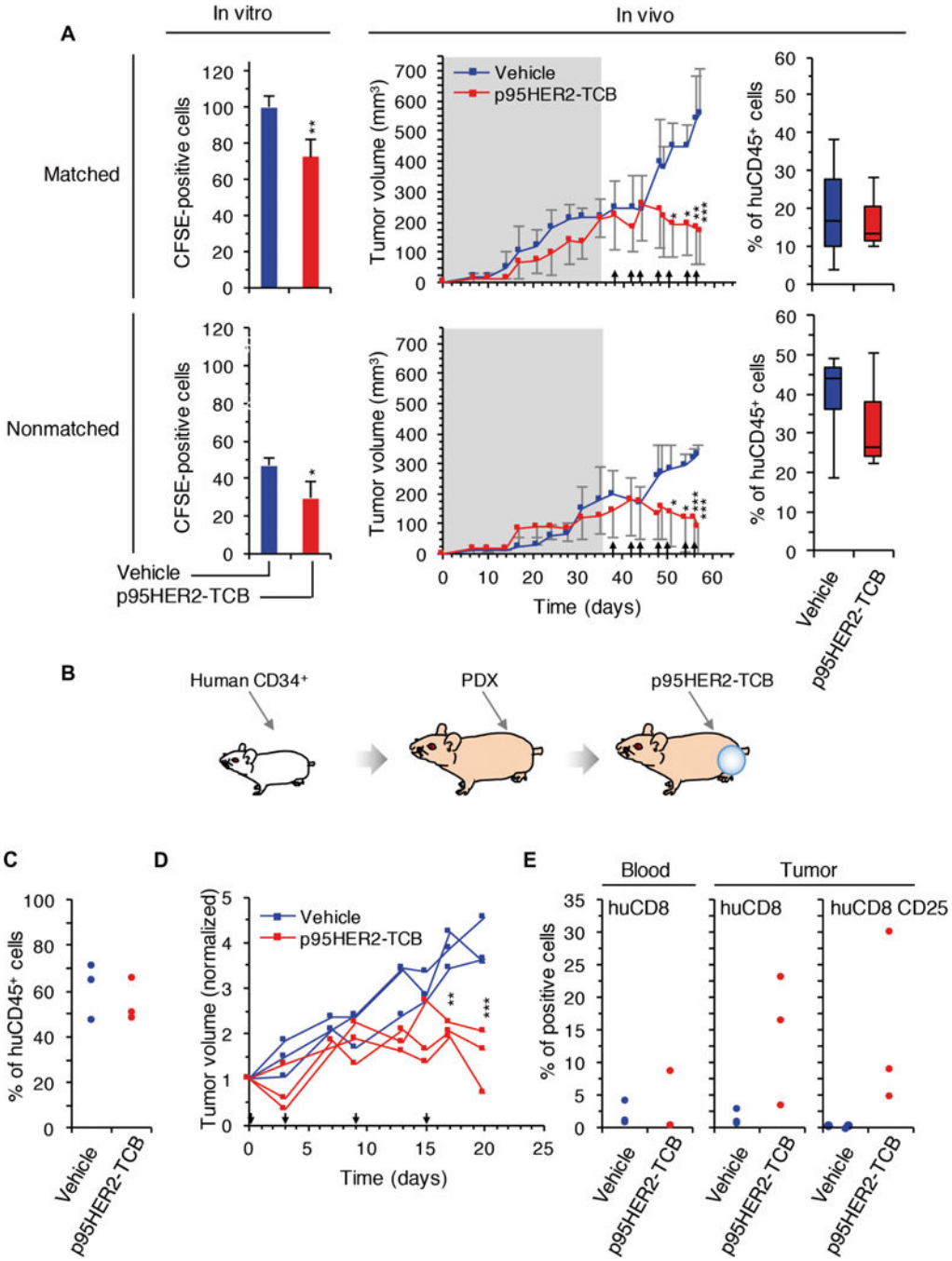

Fig. 6. Effect of p95HER2-TCB on different PDX-based models.

(**A**) In vitro, carboxyfluorescein diacetate succinimidyl ester (CFSE)–labeled primary cultures from PDX173 were incubated with PBMCs from the same patient (matched) or a healthy volunteer (nonmatched) and treated with vehicle or p95HER2-TCB. CFSE-positive cells were counted by flow cytometry. In vivo, NSG mice carrying PDX173 were monitored until tumors reached ~200 mm^3 (shadowed). Then, matched or nonmatched PBMCs were transferred. Mice were treated with vehicle or p95HER2-TCB (1 mg/kg) (arrows). Means ± SD are shown ($n \geq 3$ per group). At the end of the experiment, the percentages of circulating

human $CD45^+$ cells, relative to total leukocytes, were determined. (**B**) Schematic drawing illustrating the in vivo experiment shown in (C) to (E). (**C**) $CD34^+$ cells obtained from human cord blood were injected into 5-week-old NSG mice. After 5 months, the percentages of circulating human $CD45^+$ cells, relative to total leukocytes, were determined. (**D**) PDX173 was implanted into mice analyzed in (C). These mice were treated with vehicle or p95HER2-TCB, and tumor volume was monitored. Volumes were normalized to the volume at day 0 of treatment. (**E**) Percentages of circulating (blood, relative to total leukocytes) and intra-tumoral (tumor) human $CD8^+$ cells at the end of the experiment shown in (D). The expression of the activation marker CD25 was also analyzed in intratumor $CD8^+$ lymphocytes. $*P < 0.05$, $**P < 0.01$, $***P < 0.001$, two-way ANOVA and Bonferroni correction (A, middle, and D) and two-tailed *t* test (A, left).

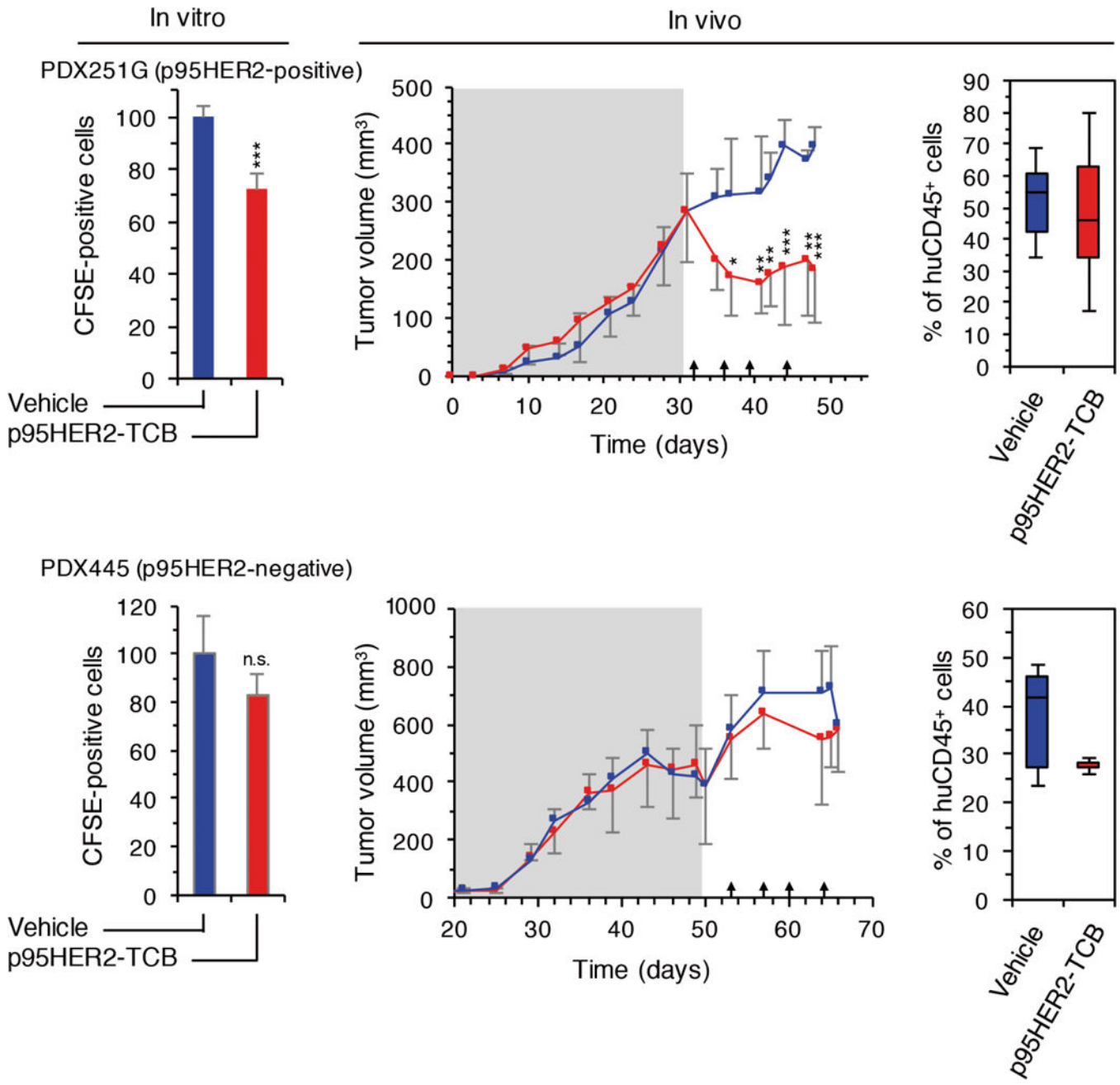

Fig. 7. Effect of p95HER2-TCB on the growth of PDXs positive and negative for p95HER2.

(**Left**) Primary cultures from PDX251G (p95HER2-positive) and PDX445 (p95HER2-negative) were treated as described in Fig. 6A with nonmatched PBMCs. (**Middle**) In vivo analyses were performed as described in Fig.6A. Means ± SD are shown ($n \geq 3$ per group). (**Right**) Percentages of circulating human $CD45^+$ cells, relative to total leukocytes, were determined at the end of the experiment. $^*P < 0.05$, $^{**}P < 0.01$, $^{***}P < 0.001$, two-tailed *t* test (left) and two-way ANOVA and Bonferroni correction (middle).